

A study of anthropogenic effect on radon emission rate

Nafis Islam Dalee¹, Sopan Das^{2*}, Minajur Rahman¹, Shafaly Khatun³, Nighat Sultana Resma², Sree Rajib Talukdar², A.K.M Rezaur Rahman¹ and Shyamal Ranjan Chakraborty¹

¹Department of Physics, University of Chittagong, Chattogram, Bangladesh; ²Atomic Energy Centre, Chattogram, Chattogram, Bangladesh; ³Radioactivity Testing and Monitoring Laboratory (RTML) Mongla, Bagerhat, Bangladesh

Abstract

Radon (^{222}Rn) is an element of significant environmental concern due to its health risks. This study examines the impact of anthropogenic activities such as urbanization, industrial emissions, and agricultural fertilizer use on radon exhalation rates and measured ^{226}Ra and ^{222}Rn concentrations in soil samples from Chattogram, Bangladesh. A total of 60 soil samples were collected from areas categorized by different human activities. The ^{226}Ra activity concentration in the first group (low human activity) ranged from 12 ± 2 to 35 ± 12 Bqkg^{-1} , in the second group (moderate activity) from 25 ± 5 to 39 ± 13 Bqkg^{-1} , and in the third group (high activity) from 30 ± 6 to 44 ± 10 Bqkg^{-1} , while ^{222}Rn concentrations in the first, second, and third groups were observed to vary from 15 ± 5 to 39 ± 9 Bqm^{-3} , 31 ± 9 to 51 ± 13 Bqm^{-3} , and 36 ± 6 to 59 ± 9 Bqm^{-3} , respectively. In high-activity areas, most locations exceed the UNSCEAR-recommended global average of 35 Bqkg^{-1} for ^{226}Ra concentrations, indicating health risks due to radium exposure in these areas. Though ^{222}Rn activity concentrations are below the recommended values suggested by ICRP, the activity concentrations have been found to increase as the locations vary from less developed to more developed areas. These findings emphasize the need for radon monitoring, mitigation measures, and public health awareness to minimize exposure risks.

Keywords: radon; natural radioactivity; radon inhalation; carcinogenic agents; radon emission

Radon (^{222}Rn) is a naturally occurring colorless and odorless gas produced by the decay of radium (^{226}Ra) which is a member of the ^{238}U series (half-life of 1,620 years) that is present in almost all rocks, building materials, and soil types. When ^{222}Rn decays to ^{218}Po , it releases an alpha particle with 5.49 MeV of energy, and these polonium atoms are metallic and have a tendency to adhere to airborne dust particles. Exposure to the decay products ^{214}Po and ^{218}Po of radon contributes over 90% to radiation doses in the human population (1, 2). ^{222}Rn has a half-life of 3.82 days. Therefore, it has enough time to travel through soil and water and enter the atmosphere by molecular diffusion, ultimately reaching the human body. The concentrations of radon vary substantially in time and location, due to varying radium concentrations in the soil and water (3).

The primary source of indoor radon exposure is the infiltration of radon gas rising from the soil or rock, making it an uncommon indoor air pollutant with a natural origin. A significant majority, at least 80%, of the radon released into the atmosphere is derived from the uppermost portions of the Earth's surface (4). As radon exposure is universal, it is found not only indoors but also

outdoors. While indoor radon concentrations tend to be higher, there is still a notable presence of radon in outdoor environments. According to data from the UK's National Radiation Protection Board, natural sources account for approximately 84% of the average annual radiation dose and the remaining 16% comes from man-made sources, with radon gas being the most significant contributor (5). Human activities can significantly impact radon exhalation by altering soil properties, disturbing radium-rich materials, and modifying natural diffusion processes. Industrial processes such as mining, quarrying, and brick manufacturing can expose radium-containing rocks, increasing the release of radon gas into the atmosphere (6, 7). Urbanization and construction activities disrupt soil layers, leading to changes in permeability and radon transport mechanisms. Building materials made from radium-bearing substances also contribute to indoor radon exposure, particularly in regions where construction materials are sourced from high-background radiation areas (8, 9). Additionally, agricultural practices, including the use of phosphate fertilizers, introduce radionuclides like uranium and radium into the soil, potentially enhancing radon emission (10, 11). Studies have shown

that areas with higher anthropogenic activity, such as industrial zones and densely populated regions, tend to exhibit elevated radon concentrations compared to rural and undisturbed locations (12). Understanding these factors is crucial for assessing the impact of human activities on environmental radioactivity and potential health risks associated with radon exposure.

Radon has been recognized as one of the group-1 carcinogenic agents as per the report of the International Agency for Research on Cancer (IARC) (13, 14). When radon progenies are inhaled, they mostly break down within the lungs due to their brief half-life and release alpha particles that can transfer substantial energy if they come into contact with the nucleus of a cell. Only a small fraction of the radon that enters the lungs has the potential to harm sensitive lung tissue by damaging DNA and leading to cancer. According to the US Environmental Protection Agency, it is the second major cause of lung cancer for smokers in the United States, and it estimated that 21,100 (about 13.4%) lung cancer deaths were radon-related out of a total of 157,400 nationally in 1995 (8, 15). Internal radon exposure may also elevate the developing health complications like leukemia and other different types of cancer, such as melanoma and cancers of the kidney and prostate (16). The National Council of Radiation Protection recommends that the annual average for indoor levels should not exceed 296 Bqm^{-3} (8 pCi/L) so as to minimize health risks (17).

In recent times, scientists have focused extensively on identifying radon due to its possible adverse effects on health and its role in environmental radioactivity. Various regions with high radon emissions, such as parts of Europe (e.g. Norway, Finland, Romania), North America, and Asia (e.g. China, India), have reported elevated radon concentrations in soil, air, and indoor environments. For instance, studies conducted in Western Norway and Romania have reported annual average indoor radon concentrations exceeding 500 Bqm^{-3} , while the arithmetic mean of radon concentrations in Finnish workplaces is approximately 91 Bqm^{-3} (18–20). In Thailand, radon concentrations in soil samples range from 5.60 to 67.10 Bqm^{-3} (21). In China, indoor and outdoor radon concentrations average 62.6 ± 44.6 and $12.9 \pm 6.3 \text{ Bqm}^{-3}$, respectively (22). These variations highlight the need for region-specific studies to assess radon exposure risks accurately.

In Bangladesh, elevated fatal cancer risk due to natural radiation exposure has been observed in the population (23). Lung cancer is one of the most common forms of the disease in the country, and the potential risk for high radon concentrations exists due to elevated radon exhalation rates (24). However, the risks of radon-induced lung cancer remain unknown due to insufficient nationwide systematic measurements. Over the past decade, some efforts have been made in various

regions of Bangladesh in conjunction with the central focus, to quantify the natural radionuclides in the soil to assess the associated radiation dose and its impact on the population (25–27). However, there has been no published research on the presence and potential effects of these radionuclides in the soils of the Satkania and Fatikchari upazila at Chattogram, Bangladesh. In order to deal with this concern, the present study focuses on measuring radon exhalation rates and associated hazard indices in soil samples from three distinct locations categorized by human activity levels (low, moderate, and high).

This study also aims to maintain national guidelines and reference data to monitor changes in environmental radioactivity caused by nuclear, industrial, and other human activities. The main objective of this project is to assess the activity concentration, radon exhalation rate, and associated hazard indices for radon present in the soil samples and the results are compared with the allowable levels worldwide. Additionally, radon concentration studies in these areas may serve as valuable indicators for forecasting geological events such as earthquakes (28, 29). Understanding the distribution and health risks of radon exposure will help in developing strategies to mitigate its impact on public health, particularly for vulnerable populations such as children. Furthermore, as the second-largest city in Bangladesh and a major port and tourist destination, Chittagong experiences significant urbanization and industrial activity, which may contribute to elevated radon exhalation. Our long-term objective is to measure the radon exhalation rate in the city and assess the associated public health hazards. The findings of this study may also serve as a foundation for future epidemiological research on radon-induced health effects in Bangladesh.

Materials and methods

Study area

The study areas are situated in the southeastern coastal region of Bangladesh, specifically in the Chattogram area. Satkania (22.1000° N , 92.0812° E) and Fatikchhari (22.7588° N , 91.7388° E) have populations of 454,062 and 642,089, respectively, covering a total area of 280.99 and 773.13 km^2 (Fig. 1). Satkania is bordered by Chandanaish Upazila to the north, Lohagara Upazila to the south, Bandarban Sadar Upazila to the east, and Banshkhali and Anwara Upazilas to the west. Fatikchhari is located between the Sitakunda Hills and the Chittagong Hill Tracts, where these two hill ranges converge at the northernmost point of the upazila and then diverge as they extend southward. It is surrounded by Tripura to the north; Hathazari, and Kawkhali Upazila to the south;

Map of study area

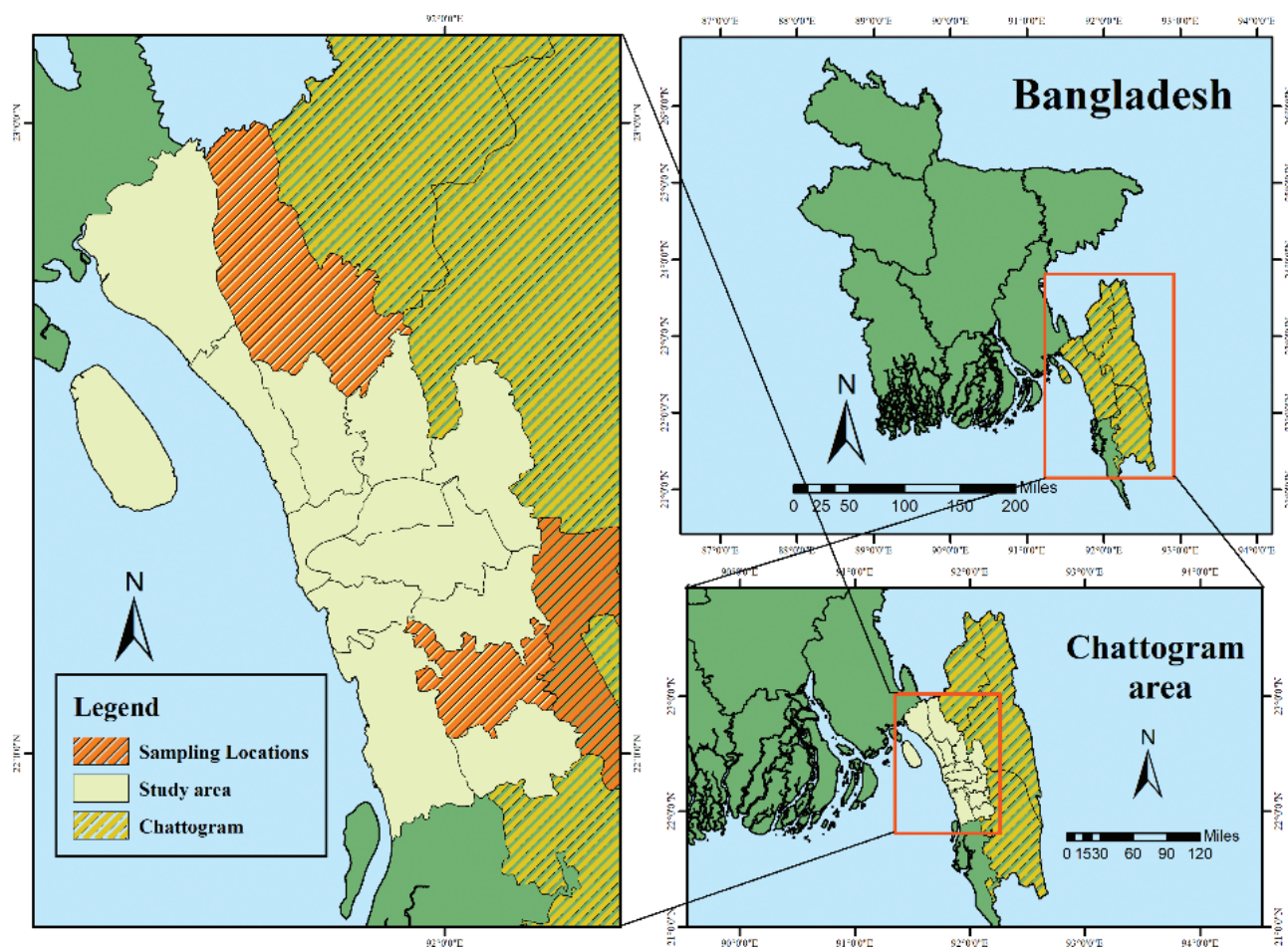


Fig. 1. Map of Chattogram including the study areas and sampling sites.

Ramgarh, Manikchhari, Lakshmichhari, and Raozan Upazilas to the east; and Mirsharai and Sitakunda Upazilas to the west.

The study areas exhibit diverse geological features and soil types, including yellowish-brown to reddish-brown loams, sandy loam, sand, and clay. These hilly regions contain croplands and tea estates. To ensure comprehensive coverage of geological variability and potential radon exhalation influences, the study area was divided into three categories based on the level of anthropogenic activities: 1) low human activity, 2) moderate human activity, and 3) high human activity. Low human activity areas represent sparsely populated, hilly regions with minimal anthropogenic interference, serving as reference locations for natural baseline radon levels. Moderate human activity areas were selected based on agricultural land use, construction sites, and moderate population density, as these factors may contribute to elevated radon exhalation due to fertilizer application and soil disturbance. Urbanized regions with high population density,

located near highways, brick kilns, and marketplaces, were chosen as high human activity sites. These areas experience significant industrial activities and vehicular emissions, which could contribute to radon variability. Additionally, Fatikchhari is a popular tourist destination, while Satkania is adjacent to Bandarban, another growing tourist hub. The increasing population and rapid tourism-driven development in these areas have led to greater anthropogenic influence, making them relevant for radon studies.

Sample collection and preparation

For this research, a total of 60 soil samples were collected from 30 sites in Satkania and Fatikchhari Upazila, Bangladesh, to ensure a representative analysis of radon exhalation rates across different levels of anthropogenic activity. Each site was selected based on its distinct geological features and level of human activity, ensuring that the study effectively captures variability in radon exhalation rates. The sample size was chosen based on

established methodologies in environmental radon studies, where sample sizes exceeding 18 are generally sufficient for robust statistical analysis and meaningful interpretation of spatial radon distribution (21, 30). The selected sites represent diverse geological features, including varying soil types, topographies, and levels of human activity, ensuring comprehensive coverage of the broader region.

Following a marking area of 4 m², roots and vegetation contained in the top layer of soil were removed and two specimens were taken from each location – one from the surface and another from a depth of about 30 cm with the help of a soil auger. Then the collected samples were carefully preserved in separate sealable plastic bags to prevent any types of deterioration or contamination.

Water can promote radon exhalation up to a certain moisture level, but once the water content exceeds a threshold, it instead traps more radon, thereby restraining exhalation. Previous studies have found that radon exhalation rates tend to decrease steadily when soil moisture exceeds 8% (31). In many studies, it is also observed that the radon exhalation rate is strongly influenced by the moisture and temperature of the soil and the exhalation rate is higher during the summer season, owing to variations in soil moisture that influence the seasonal fluctuations in soil air radon concentration (32, 33). To minimize the influence of these environmental variables (rainfall and temperature) all measurements were conducted in November and December (dry season), ensuring consistency across samples and dried soil samples were used to further control the effects of moisture content. The specimens were initially air-dried for several days to allow the moisture content to evaporate and dried in an oven at 105°C for 24 h to remove the remaining moisture. All the large stones or debris were removed from the samples and crushed using a mortar and pestle. Following this, the soil samples were then sieved using a 75 mm mesh size to obtain a homogeneous powder and ensure a representative composition for analysis. After measuring the net weight, the resulting soil samples were stored in airtight containers to prevent any contamination or loss of radioactivity. These samples were stored for about 30 days to allow ²²²Rn to reach a secular equilibrium with their respective daughter radionuclides.

Gamma analysis

To measure the concentration of ²²⁶Ra in the soil samples through gamma analysis, a high-purity Germanium (HPGe) detector was used. The study was conducted using the gamma-ray spectrometry facilities at the Atomic Energy Centre, Chattogram, Bangladesh. The NATS-2 2465-17 HPGe detector with a relative efficiency of 40% at 1.33 MeV photon concerning 3"×3" NaI detector and Co-60 source was mounted 25 cm above the detector.

The detector's efficiency calibration was done using standard soil-327 from the International Atomic Energy Agency (IAEA). The spectrum for ²²⁶Ra was analyzed using Canberra Genie-2000 software. After efficiency calibration, each soil samples are counted for 30,000 s in the HPGe detector system.

RadonEye Plus2 device

In this work, a RadonEye Plus2 device was used in the closed chamber method to measure the ²²²Rn concentration in the air (8). This approach is designed to simulate controlled conditions, similar to indoor environments, by enclosing soil samples in a sealed chamber.

The RadonEye Plus2 is an electronic radon monitoring device with high sensitivity based on a pulsed ionization chamber sensor to detect radon gas precisely. It measures radon concentrations from 3.7 to 9,435 Bqm⁻³ (0.1 pCi/L to 255 pCi/L) with 10% accuracy at 3,700 Bqm⁻³ (10 pCi/L) after 1 h. The device provides initial readings in 10 min and continuous hourly updates. It supports Bluetooth and Wi-Fi for real-time monitoring via mobile apps and stores up to 1 year of data, allowing users to track radon levels over extended periods without manual recording. The RadonEye Plus2 is powered by an AC adapter with optional battery backup, the device features an Organic Light-Emitting Diode (OLED) display for immediate radon level readings. It operates effectively within a temperature range of 0–40°C and 0–80% humidity (34, 35). Additionally, RadonEye Plus2 has a portable and compact design, making it easy to move between locations without specialized installation or maintenance. It is factory-calibrated and ready for immediate use, reducing complexity for non-expert users.

Radon collection system

A square plastic box ($V_c = 0.283 \text{ m}^3$) with an airtight lid was taken to create a controlled environment for radon gas measurement as shown in Fig. 2. The box remained closed for 2 weeks to let the radon gas reach saturation and decay any background radon, allowing for more accurate measurements of the radon levels in the sample. A sample was spread on a tray ($A = 0.371 \text{ m}^2$) to disperse particles thinly over the surface. Later, it was enclosed at the bottom in the airtight plastic box with the radon detector placed on a stand and a fan in the corner for gas circulation. The detector was then powered on and paired with a smartphone running the Radon Eye application via Bluetooth to enable real-time monitoring of radon levels at 10-min intervals. Longer exposure times lead to more stable readings and allow radon concentrations to accumulate within the chamber, making detection easier and accurate. We maintained the soil in the chamber for 36 h and recorded the radon concentrations in Bqm⁻³.

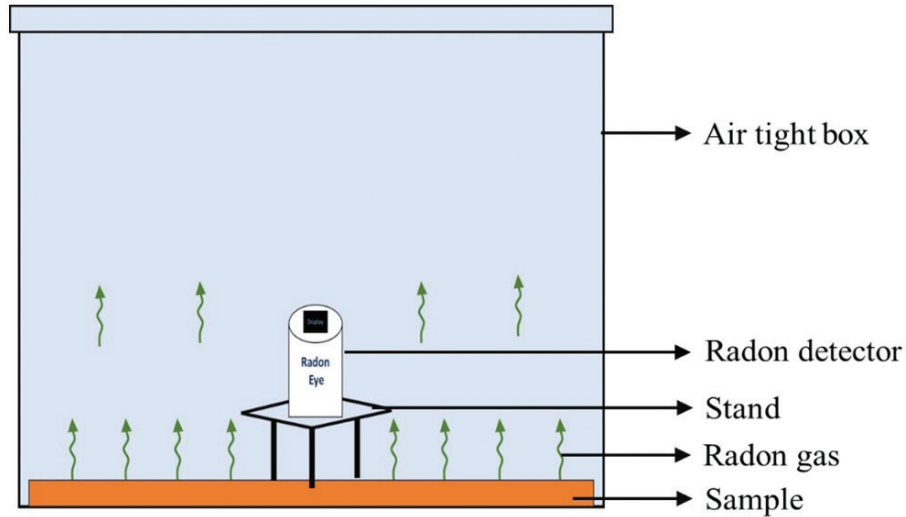


Fig. 2. Schematic diagram of radon measurement.

Radon exhalation rate

The radon exhalation rate, Exh ($\text{Bqm}^{-2}\text{h}^{-1}$) of the sample was determined utilizing the formula defined in the equations (36, 37)

$$\text{Exh} = \frac{\lambda V_c}{A} \times A_{\text{Rn}} \tag{1}$$

Here, $\lambda = \frac{0.693}{T_{1/2}}$ (2)

and $T_{1/2}$ = Half-life of radon = 3.82 days

Where:

- λ_{eff} = Decay constant of radon (h^{-1})
- V_c = Volume of the chamber (m^3)
- A_{Rn} = Outdoor radon concentration (Bqm^{-3}) and
- A = Surface area (m^2)

Therefore, substituting the values to the equation (1) as mentioned earlier gives,

$$\text{Exh} (\text{Bqm}^{-2}\text{h}^{-1}) = 0.005766 \times A_{\text{Rn}} \tag{3}$$

Assessment of radiological hazard

To estimate the annual effective dose due to radon, D_{Rn} (mSvy^{-1}) in the air, the conversion coefficient from the absorbed dose in the air to the effective dose received by an individual must be considered. This value was published in the UNSCEAR 2000 report as 9 nSv per Bqhm^{-3} for environmental exposure to radon levels. The annual effective dose received by the public, D_{Rn} (mSvy^{-1}) was measured by using the following equation (38)

$$D_{\text{Rn}} = A_{\text{Rn}} \times F_{\text{eq}} \times T \times \text{DCF} \tag{4}$$

where:

- D_{Rn} = Annual effective dose (mSvy^{-1})
- A_{Rn} = Outdoor radon concentration (Bqm^{-3})
- F_{eq} = Equilibrium factor (typically 0.6 for outdoors) between radon and its progeny
- T = Occupancy time (1,760 h per year for outdoors) and
- DCF = Dose conversion factor (9 nSv per Bqhm^{-3}) for radon exposure

Therefore,

$$D_{\text{Rn}} (\text{mSvy}^{-1}) = A_{\text{Rn}} (\text{Bqm}^{-3}) \times 0.6 \times 1,760 \frac{\text{h}}{\text{year}} \times 9 \times 10^{-6} \frac{\text{mSv}}{\text{Bqhm}^{-3}} \tag{5}$$

Results & discussion

The measured values of ^{226}Ra activity concentration and ^{222}Rn exhalation rate for three levels of human activity: low, moderate, and high of 60 soil samples collected from Satkania and Fatikchari in Bangladesh are tabulated in Table 1.

In low-activity areas, ^{226}Ra concentration (A_{Ra}) varied between the minimum and maximum values of 12 ± 2 to $35 \pm 12 \text{ Bqkg}^{-1}$ with a mean value of $23.495 \pm 6.60 \text{ Bqkg}^{-1}$. Moderate-activity areas exhibited a higher range, between 25 ± 5 and $39 \pm 13 \text{ Bqkg}^{-1}$ with an average of $29.810 \pm 6.65 \text{ Bqkg}^{-1}$. High-activity areas displayed the highest concentrations, ranging from 30 ± 6 to $44 \pm 10 \text{ Bqkg}^{-1}$, with an average of $35.0 \pm 8.4 \text{ Bqkg}^{-1}$. These values are consistent with global averages, except for the high-activity areas, where most locations exceed the worldwide median of 35 Bqkg^{-1} recommended by UNSCEAR (38). The results indicate that this area is not safe concerning the health hazards associated with radium exposure.

As shown in Table 2, the radon concentration (A_{Rn}) also increases with human activity. In low-activity areas,

Table 1. The activity concentration of ^{226}Ra (A_{Ra}) and ^{222}Rn exhalation rate (E_x) in soil samples

Surface level	Low human activity			Moderate human activity			High human activity		
	Sample ID	^{226}Ra (Bqkg ⁻¹)	E_x (Bqm ⁻² h ⁻¹)	Sample ID	^{226}Ra (Bqkg ⁻¹)	E_x (Bqm ⁻² h ⁻¹)	Sample ID	^{226}Ra (Bqkg ⁻¹)	E_x (Bqm ⁻² h ⁻¹)
Surface level	BCS-1	12.6 ± 2	0.086	BCS-11	28.9 ± 7	0.208	BCS-21	44.1 ± 10	0.306
	BCS-2	28.9 ± 9	0.208	BCS-12	31.5 ± 10	0.242	BCS-22	35.4 ± 11	0.259
	BCS-3	18.1 ± 5	0.150	BCS-13	38.9 ± 13	0.294	BCS-23	35.1 ± 8	0.254
	BCS-4	17.5 ± 5	0.127	BCS-14	31.2 ± 7	0.236	BCS-24	42.7 ± 13	0.340
	BCS-5	25.1 ± 6	0.213	BCS-15	29.9 ± 6	0.225	BCS-25	40.6 ± 12	0.277
	BCS-6	26.7 ± 5	0.185	BCS-16	28.1 ± 6	0.213	BCS-26	39.7 ± 11	0.311
	BCS-7	25.4 ± 7	0.173	BCS-17	29.3 ± 6	0.225	BCS-27	33.7 ± 7	0.236
	BCS-8	26.6 ± 8	0.185	BCS-18	30.1 ± 6	0.213	BCS-28	32.2 ± 7	0.248
	BCS-9	34.6 ± 12	0.208	BCS-19	28.5 ± 5	0.219	BCS-29	31.1 ± 7	0.231
	BCS-10	19.8 ± 5	0.138	BCS-20	32.1 ± 7	0.219	BCS-30	32.4 ± 7	0.225
30 cm depth	BCD-1	15.9 ± 3	0.144	BCD-11	26 ± 6	0.179	BCD-21	33.7 ± 9	0.242
	BCD-2	22.6 ± 6	0.219	BCD-12	25.2 ± 5	0.185	BCD-22	31.5 ± 6	0.219
	BCD-3	18.5 ± 5	0.173	BCD-13	28.5 ± 9	0.213	BCD-23	30.6 ± 5	0.208
	BCD-4	18.1 ± 5	0.167	BCD-14	31.2 ± 6	0.236	BCD-24	38.9 ± 11	0.306
	BCD-5	22.1 ± 9	0.185	BCD-15	29.9 ± 6	0.225	BCD-25	38.2 ± 11	0.288
	BCD-6	29.2 ± 5	0.225	BCD-16	28.1 ± 5	0.213	BCD-26	37.2 ± 10	0.277
	BCD-7	27.7 ± 8	0.208	BCD-17	29.3 ± 5	0.213	BCD-27	32.2 ± 6	0.213
	BCD-8	30.8 ± 11	0.213	BCD-18	30.1 ± 6	0.208	BCD-28	30.8 ± 6	0.213
	BCD-9	29.1 ± 9	0.219	BCD-19	29.3 ± 6	0.213	BCD-29	30.1 ± 6	0.225
	BCD-10	20.6 ± 7	0.150	BCD-20	30.1 ± 6	0.213	BCD-30	30.4 ± 6	0.219
Average of ^{226}Ra Concentration	Low human activity				23.495 ± 6.60 Bqkg ⁻¹				
	Moderate human activity				29.810 ± 6.65 Bqkg ⁻¹				
	High human activity				35.030 ± 8.45 Bqkg ⁻¹				

radon concentrations ranged from 15 ± 5 to 39 ± 9 Bqm⁻³, with an average of 31 ± 8.6 Bqm⁻³. Moderate-activity areas had values between 31 ± 9 and 51 ± 13 Bqm⁻³, averaging 38.1 ± 8.1 Bqm⁻³. High-activity areas recorded the highest radon levels, ranging from 36 ± 6 to 59 ± 9 Bqm⁻³, with a mean of 44.2 ± 8.6 Bqm⁻³. Despite this variation, all measured radon

concentrations remain below the recommended safe range set by ICRP (200–600 Bqm⁻³) and WHO (100 Bqm⁻³) (39–41).

The findings suggest that the concentrations of ^{222}Rn and ^{226}Ra in soil samples varied notably across different sampling locations. This variability may be attributed to both natural geological differences and

Table 2. Radiation hazard index due to radon in three distinguished groups of areas

Low human activity				Moderate human activity				High human activity			
Sample ID	²²² Rn (Bqm ⁻³)	E _x (Bqm ⁻² h ⁻¹)	D _{Rn} (mSvy ⁻¹)	Sample ID	²²² Rn (Bqm ⁻³)	E _x (Bqm ⁻² h ⁻¹)	D _{Rn} (mSvy ⁻¹)	Sample ID	²²² Rn (Bqm ⁻³)	E _x (Bqm ⁻² h ⁻¹)	D _{Rn} (mSvy ⁻¹)
BCS-1	15 ± 5	0.086	0.143	BCS-11	36 ± 10	0.208	0.342	BCS-21	53 ± 13	0.306	0.504
BCS-2	36 ± 10	0.208	0.342	BCS-12	42 ± 11	0.242	0.399	BCS-22	45 ± 13	0.259	0.428
BCS-3	26 ± 7	0.150	0.247	BCS-13	51 ± 13	0.294	0.485	BCS-23	44 ± 7	0.254	0.418
BCS-4	22 ± 6	0.127	0.209	BCS-14	41 ± 7	0.236	0.390	BCS-24	59 ± 9	0.340	0.561
BCS-5	37 ± 10	0.213	0.352	BCS-15	39 ± 7	0.225	0.371	BCS-25	48 ± 9	0.277	0.456
BCS-6	32 ± 9	0.185	0.304	BCS-16	37 ± 7	0.213	0.352	BCS-26	54 ± 9	0.311	0.513
BCS-7	30 ± 9	0.173	0.285	BCS-17	39 ± 7	0.225	0.371	BCS-27	41 ± 8	0.236	0.390
BCS-8	32 ± 9	0.185	0.304	BCS-18	37 ± 7	0.213	0.352	BCS-28	43 ± 9	0.248	0.409
BCS-9	36 ± 9	0.208	0.342	BCS-19	38 ± 7	0.219	0.361	BCS-29	40 ± 8	0.231	0.380
BCS-10	24 ± 6	0.138	0.228	BCS-20	38 ± 7	0.219	0.361	BCS-30	39 ± 8	0.225	0.371
BCD-1	25 ± 10	0.144	0.238	BCD-11	31 ± 9	0.179	0.295	BCD-21	42 ± 12	0.242	0.399
BCD-2	38 ± 9	0.219	0.361	BCD-12	32 ± 9	0.185	0.304	BCD-22	38 ± 9	0.219	0.361
BCD-3	30 ± 9	0.173	0.285	BCD-13	37 ± 11	0.213	0.352	BCD-23	36 ± 6	0.208	0.342
BCD-4	29 ± 9	0.167	0.276	BCD-14	41 ± 7	0.236	0.390	BCD-24	53 ± 8	0.306	0.504
BCD-5	32 ± 10	0.185	0.304	BCD-15	39 ± 7	0.225	0.371	BCD-25	50 ± 8	0.288	0.475
BCD-6	39 ± 9	0.225	0.371	BCD-16	37 ± 7	0.213	0.352	BCD-26	48 ± 7	0.277	0.456
BCD-7	36 ± 10	0.208	0.342	BCD-17	37 ± 7	0.213	0.352	BCD-27	37 ± 7	0.213	0.352
BCD-8	37 ± 10	0.213	0.352	BCD-18	36 ± 7	0.208	0.342	BCD-28	37 ± 7	0.213	0.352
BCD-9	38 ± 6	0.219	0.361	BCD-19	37 ± 7	0.213	0.352	BCD-29	39 ± 7	0.225	0.371
BCD-10	26 ± 9	0.150	0.247	BCD-20	37 ± 7	0.213	0.352	BCD-30	38 ± 7	0.219	0.361
Average	31 ± 8.55	0.179	0.295	Average	38.1 ± 8.05	0.220	0.362	Average	44.2 ± 8.55	0.255	0.420
²²²Rn concentration range	Low			15 ± 5 – 39 ± 9 Bqm ⁻³							
	Moderate			31 ± 9 – 51 ± 13 Bqm ⁻³							
	High			36 ± 6 – 59 ± 9 Bqm ⁻³							

anthropogenic influences. In highly populated areas, activities such as brick kilns, tea estates with intensive fertilizer use, construction, industrialization, and heavy traffic emissions may disrupt soil composition, promoting radon diffusion into the atmosphere.

Additionally, geochemical processes occurring within the soil or the geogenic factors, particularly soil properties, likely play a significant role in the variation in radon concentrations (42, 43). It is noteworthy that the radon concentration data at two different depths were

quite similar, which may be due to the uniformity of soil types at the sampling locations. This observed similarity in radon concentrations at different depths can contribute to indoor radon mapping, especially in areas with similar soil properties. Since radon transport is not significantly depth-dependent in this region, radon levels may be more influenced by surface permeability, soil moisture, and weather conditions rather than subsurface variations. This insight can help refine radon mapping strategies by focusing on surface conditions in risk assessments. Future studies incorporating detailed geochemical analyses on soil could provide a more comprehensive understanding of how natural and anthropogenic factors interact to influence radon dynamics. Integrating our measured radon exhalation rates, and ^{226}Ra activity, and future studies on soil characteristics can contribute to developing a radon potential map for Chattogram. This would be valuable for regional risk assessments, land-use planning, and public health interventions, as proposed in previous works (44).

The radon exhalation rate (E_x) was determined in this study using Equation 3 and is also shown in Table 2.

The mean exhalation rates for low, moderate, and high human activity areas were 0.179, 0.220, and

0.255 $\text{Bqm}^{-2}\text{h}^{-1}$, respectively, which are well below the global average of $0.016 \text{ Bqm}^{-2}\text{s}^{-1}$ ($57.6 \text{ Bqm}^{-2}\text{h}^{-1}$) as reported by UNSCEAR (38). Overall, the study confirms that the soil gas radon in the study area, along with the associated radon exhalation, does not pose any significant health risk to humans.

Statistical analysis

To assess the normality of the datasets, the Shapiro–Wilk test was performed, and the histogram plot in Fig. 3 shows the data distribution along with KDE (Kernel Density Estimate) curves for each dataset. In Table 3, the results indicate that radium concentrations in moderate and high activity areas, as well as radon concentrations in moderate activity areas, deviate from a normal distribution ($P < 0.05$).

Given this mixed normality behavior, the non-parametric Kruskal–Wallis test was performed (Table 3). The Kruskal–Wallis test revealed statistically significant differences in radium ($H = 37.06, P = 8.96 \times 10^{-9}$) and radon ($H = 30.91, P = 1.94 \times 10^{-7}$) concentrations among the three activity levels. These results suggest that human activities significantly influence the distribution of radium and radon in the studied areas and the differences in ^{226}Ra and ^{222}Rn concentrations across

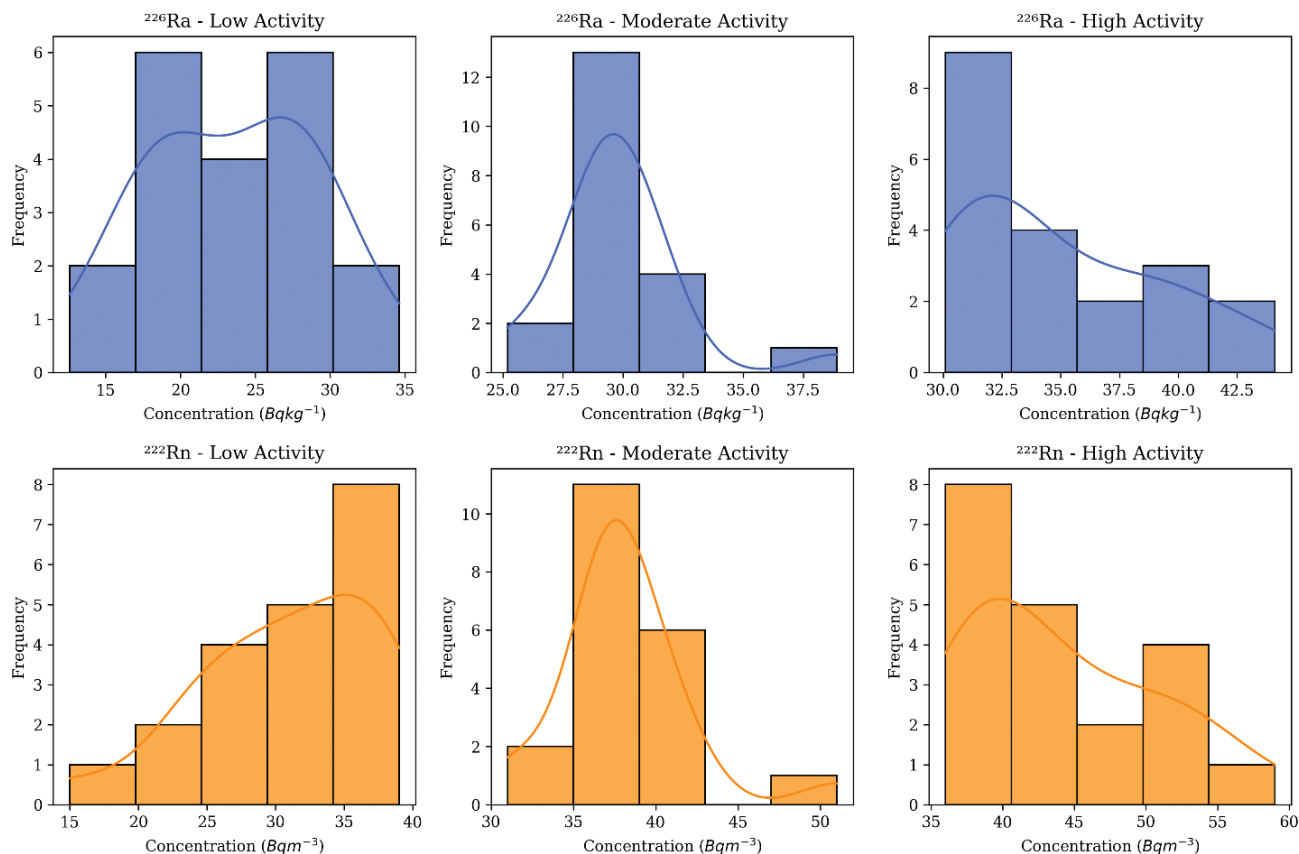


Fig. 3. The histogram with normal distribution curves for both ^{226}Ra and ^{222}Rn concentrations across different activity levels.

Table 3. Results of Shapiro–Wilk tests and Kruskal–Wallis test

Parameter	Human activity level	Shapiro-Wilk test result			Kruskal-Wallis test result		
		Test Statistic	P	Normality	Test Statistic, H	P	Statistical Significance
²²⁶ Ra Concentration	Low	0.974	0.829	Normal	37.06	8.96×10^{-9}	Significant
	Moderate	0.831	0.0026	Not Normal			
	High	0.902	0.0448	Not Normal			
²²² Rn Concentration	Low	0.923	0.113	Normal	30.91	1.94×10^{-7}	Significant
	Moderate	0.829	0.0025	Not Normal			
	High	0.915	0.0811	Normal			

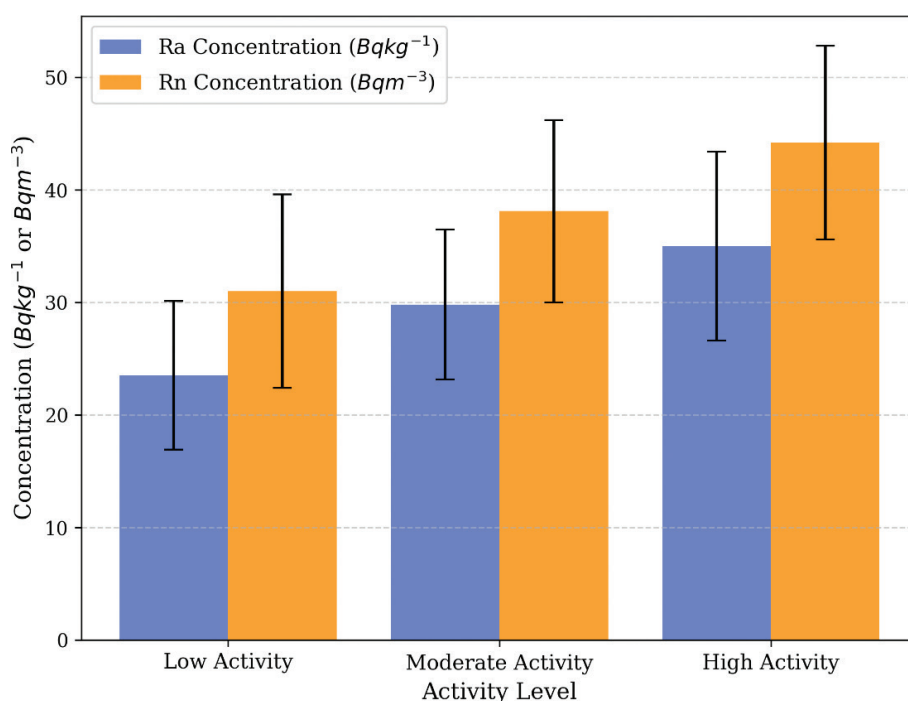


Fig. 4. A bar chart comparing Ra and Rn concentrations across different activity levels with error bars indicating uncertainty.

the three activity groups (low, moderate, and high) are shown in Fig. 4.

Correlation analysis

To quantify the relationship between radium and radon concentrations, linear regression analyses were conducted separately for each activity level.

As illustrated in Figs. 5–7, a strong positive correlation between Radium Concentration (Bqkg⁻¹) and Radon Concentration (Bqm⁻³) was observed, with R^2 values of 0.708, 0.867, and 0.879 for low, moderate, and high activity areas, respectively. Additionally, the P -value below 0.05 for all the activity areas suggests that the relationship is statistically significant. This indicates that the

radium content in the soil is the primary source of radon in these environments, consistent with established radiological principles. The stronger correlations in areas of moderate and high human activity suggest that human activities, such as intensive farming, construction, burning fossil fuels, and traffic, may enhance radium release into the air.

Radiological hazard assessment

The annual effective dose due to radon inhalation (D_{Rn}) was estimated using Equation 5. As shown in Table 2, the average doses for low, moderate, and high activity areas are 0.295, 0.362, and 0.420 mSv⁻¹, respectively. The estimated annual effective doses

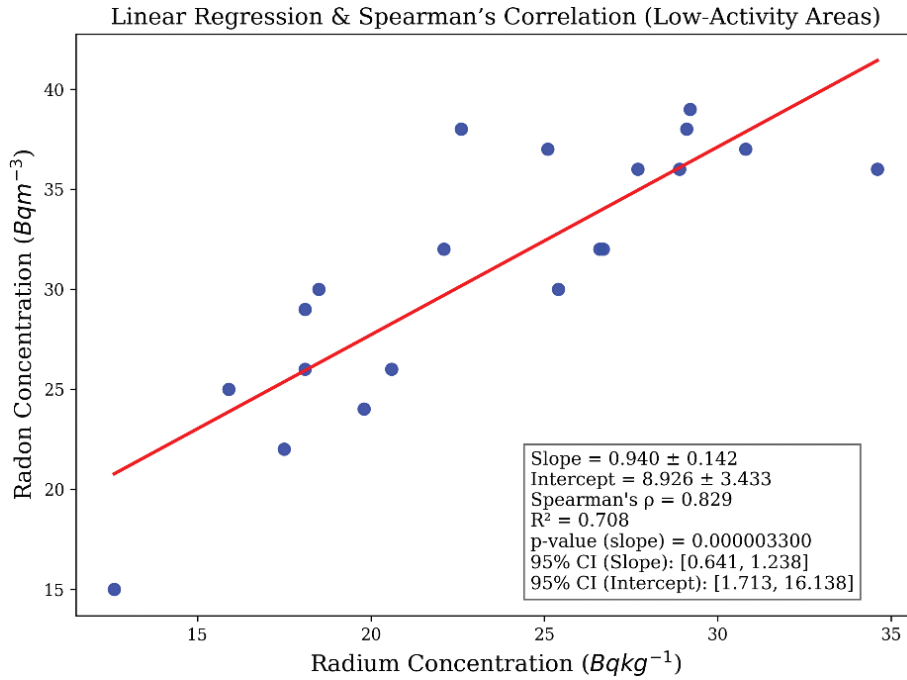


Fig. 5. Correlation Between Radium and Radon concentration in low-activity areas.

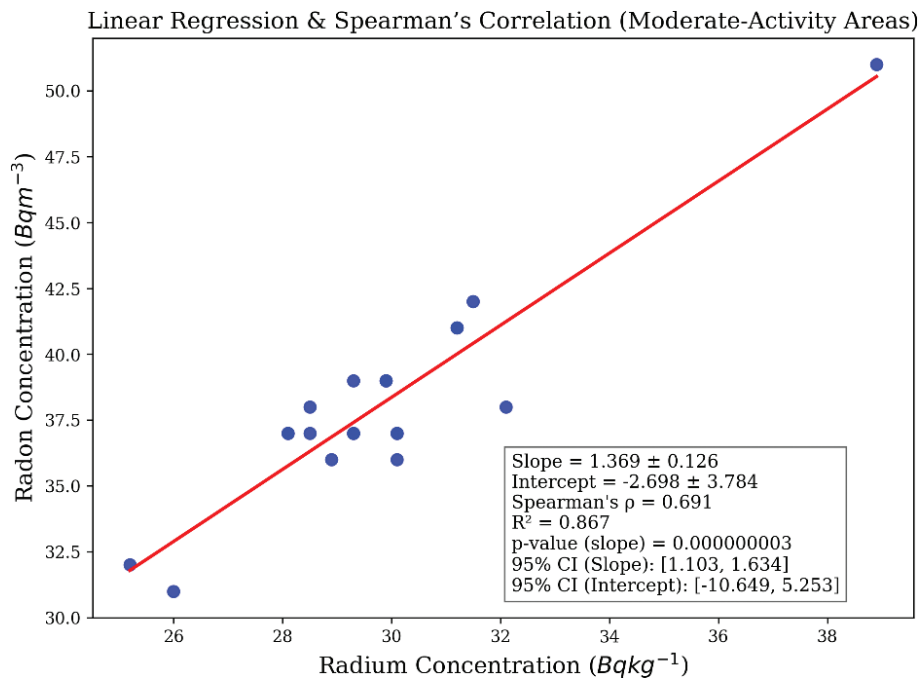


Fig. 6. Correlation Between Radium and Radon concentration in moderate-activity areas.

due to radon inhalation are lower than the permissible limit of $1 \text{ mSv}\cdot\text{y}^{-1}$ according to the ICRP recommendation (38). Although all calculated annual effective doses remain below regulatory limits, prolonged exposure to even low levels of radon poses potential long-term health risks, particularly for

vulnerable populations such as children, the elderly, and individuals with pre-existing health conditions.

The results obtained in this study have been compared with previously reported values from various locations in Bangladesh, including Kuakata and Cox's Bazar, as

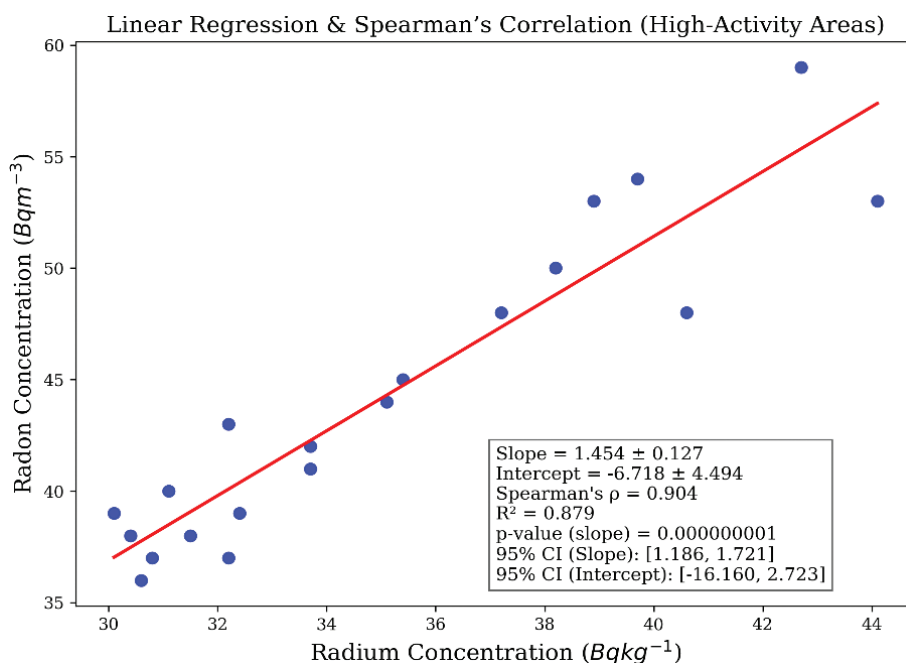


Fig. 7. Correlation Between Radium and Radon concentration in high-activity areas.

Table 4. Comparison of measured radon concentration and the radon exhalation rate with published data from worldwide and research conducted in a few other areas in Bangladesh

Location	Depth (cm)	Detector type	Radon concentration (Bqm ³)	Radon exhalation rate (Bqm ² h ⁻¹)	References
Garhwal Himalaya, India	25, 30, 35	Smart RnDuo	9 ± 1 – 680 ± 95	3 ± 0.7 to 98 ± 3	(45)
Perak State, Malaysia	80	RAD7	0.11 – 434.5 (kBqm ⁻³)	-	(46)
West Nile Delta, Egypt	-	CR-39	236.34 – 717.78	0.28 to 0.86	(47)
Al-Qassim, Saudi Arabia	Surface, 60	AlphaGUARD PQ2000 PRO	26 ± 5 – 340 ± 22	-	(48)
Al-Diwaniyah, Iraq	Surface, 10, 20, 30, and 40	CR-39	163.6 – 689.9	0.015 to 0.063	(49)
Rajasthan, India	10, 40, 70, and 100	RAD7	0.09 – 10.40	-	(50)
Thiqr, Iraq	Surface and 10	CR-39	75.875 ± 21.80	33.003 to 139.103 (mBqm ² h ⁻¹)	(51)
AL-Qadisiyah, Iraq	5 to 15	CR-39	83.14 – 323.95	0.021–0.083 (mBqm ² h ⁻¹)	(52)
Kuakata, Bangladesh	Surface, 20 and 40	AlphaGUARD PQ2000 PRO	10 ± 4 – 4790 ± 51	-	(53)
Cox's Bazar, Bangladesh	20, 40 and 60	AlphaGUARD PQ2000 PRO	132 ± 20 to 66,800 ± 2108	-	(54)
Satkania & Fatikchari, Bangladesh	Surface and 30	RadonEye Plus 2	15 ± 5 – 59 ± 9	0.086 to 0.34	Present study

presented in Table 4. Additionally, international studies on soil radon concentrations from India, Malaysia, Egypt, Saudi Arabia, and Iraq have been included. The present study reports lower values than those in Kuakata and Cox's Bazar, Bangladesh, but higher

values than those recorded in Garhwal Himalaya, India; Perak State, Malaysia; West Nile Delta, Egypt; Al-Qassim, Saudi Arabia; Thiqr, Iraq; and Al-Diwaniyah, Iraq. Notably, the radon concentration in Rajasthan, India, is significantly lower than in other

cities and countries. These variations may be attributed to differences in soil depth, anthropogenic activities, detection techniques, and geological characteristics.

Limitations

The study was conducted on soil samples from specific sites within Satkania and Fatikchari Upazilas. While the selected sites were categorized by human activity levels, the sampling may not fully capture the variability in radon emissions across a broader area. Additionally, key environmental factors like soil moisture, temperature, and atmospheric pressure, which can influence radon exhalation, were not analyzed in detail. The closed-chamber technique minimized environmental impacts during measurements, but year-round sampling, detailed soil analysis, and atmospheric monitoring are recommended for future studies. Furthermore, health risk assessments were based on standard conversion factors rather than direct epidemiological data. Despite these constraints, the findings offer valuable baseline data, and future research with extended monitoring and broader sampling will help refine risk assessments and mitigation strategies.

Conclusion

This study demonstrates the fact that human activities significantly influence radium (^{226}Ra) and radon (^{222}Ra) concentrations in soil across Satkania and Fatikchari, Bangladesh. The findings reveal a consistent increase in radium and radon levels with higher anthropogenic activity, with statistical analysis confirming significant differences among low, moderate, and high-activity areas. The strong positive correlation between radium and radon concentrations suggests that land-use changes, industrial activities, and increased vehicular emissions contribute to elevated radon emissions. Although the measured radon concentrations remain below internationally recommended safety limits, prolonged exposure, particularly in high-activity zones, may pose long-term health risks, including an increased likelihood of lung cancer. Children may still be susceptible to the effects of the observed radon exhalation level due to their thin skin and high breathing frequency. Therefore, proactive mitigation strategies are essential to minimize radon exposure risks. Policymakers should implement radon mitigation measures such as improved ventilation in buildings, radon-resistant construction techniques, and retrofitting existing structures with radon barriers. Public health awareness campaigns are also necessary to educate communities about the risks of radon inhalation and encourage radon testing in homes, workplaces, and schools. Additionally, regular monitoring and regulatory updates, including region-specific safety standards aligned with international guidelines, should be enforced to manage exposure risks effectively. Further research, including expanded radon

surveys across different regions and seasons, incorporating soil geochemistry and meteorological factors, would enhance the understanding of radon behavior. Developing a radon potential map for Chattogram could serve as a vital tool for risk assessment and targeted mitigation efforts. By adopting these measures, policymakers can minimize health risks, ensure safer urban expansion, and promote sustainable land-use planning in rapidly developing areas. Overall, the data gathered through this research will help establish a comprehensive reference database, enabling the identification of future changes due to geogenic and anthropogenic activities and the implementation of radiation safety measures. The data may aid in the identification of radon sources and the development of nationwide mapping of radon.

Conflict of interest and funding

No funding was received for this study.

The Authors declare that they have no known competing financial interests or personal relationships that could have appeared to influence the work reported in this paper.

References

1. Gruber V, Maringer FJ, Landstetter C. Radon and other natural radionuclides in drinking water in Austria: measurement and assessment. *Appl Radiat Isot* 2009; 67(5): 913–7. doi: 10.1016/j.apradiso.2009.01.056
2. United Nations Scientific Committee on the Effects of Atomic Radiation. Sources, effects, and risks of ionizing radiation report to the general assembly with annexes. New York: United Nations Publications; 1994.
3. UNSCEAR. Sources and effects of ionizing radiation. New York: International Journal of Radiation Biology; 1993.
4. UNSCEAR. Sources and effects of ionizing radiation. Report to General Assembly with Scientific Annexes. New York: United Nations; 2008.
5. Oatway WB, Jones AL, Holmes S. Ionising radiation exposure of the UK population, 2010 review. Centre for Radiation, Chemical and Environmental Hazards. Chilton, Didcot, Oxfordshire: Public Health England; 2016.
6. Naftz DL, Walton-Day K, Gardner WP, Duniway MC, Bills D. Natural and anthropogenic processes affecting radon releases during mining and early stage reclamation activities, Pinenut uranium mine, Arizona, USA. *J Environ Radioactivity* 2020; 220: 106266. doi: 10.1016/j.jenvrad.2020.106266
7. Cho J-H, Dong K-R, Ju Y-J, Chung W-K, Kim S-C, Lee J-W, et al. A study on measurement and analysis of radon-222 (uranium series) emitted to the atmosphere from construction materials (cement block, kaolin brick, and gypsum board) in living environment. *Environ Earth Sci* 2013; 70: 1515–23. doi: 10.1007/s12665-013-2238-x
8. Das S, Hossain S. Radon exhalation and health hazard assessment for various ceramic tiles used in Bangladesh. *Journal of the European Radon Association* 2024; 5: 10473. doi: 10.35815/radon.v5.10473.
9. Kovler K. Radon exhalation of hardening concrete: monitoring cement hydration and prediction of radon concentration in construction site. *J Environ Radioact* 2006; 86(3): 354–66. doi: 10.1016/j.jenvrad.2005.10.005

10. Kaur I, Gupta A, Singh BP, Sharma S, Kumar A. Assessment of radon and potentially toxic metals in agricultural soils of Punjab, India. *Microchem J* 2019; 146: 444–54. doi: 10.1016/j.microc.2019.01.028
11. Kadi MW, Al-Eryani DA. Natural radioactivity and radon exhalation in phosphate fertilizers. *Arabian Journal for science and Engineering* 2012; 37:225-31. doi: 10.1007/s13369-011-0156-3
12. Čujić M, Janković Mandić L, Petrović J, Dragović R, Đorđević M, Đokić M, et al. Radon-222: environmental behavior and impact to (human and non-human) biota. *Int J Biometeorol* 2021; 65: 69–83.
13. IARC (International Agency for Research on Cancer). Monographs on the evaluation of carcinogenic risks to humans. In: Man made mineral fibres and radon. Lyon, France: World Health Organization, 1988; p. 43.
14. Duggal V, Mehra R, Rani A. Study of radium and radon exhalation rate in soil samples from areas of Northern Rajasthan. *J Geol Soc India* 2015; 86: 331–6. doi: 10.1007/s12594-015-0319-z
15. EPA assessment of risks from radon in homes. Washington, DC: Off Radiat Indoor Air, United States Environ Prot Agency; 2003.
16. Henshaw DL, Eatough JP, Richardson RB. Radon as a causative factor in induction of myeloid leukemia and other cancers. *Lancet* 1990; 335(8696): 1008–12. doi: 10.1016/0140-6736(90)91071-H
17. National Research Council, Commission on Life Sciences, Board on Radiation Effects Research, and Committee on Health Risks of Exposure to Radon (BEIR VI). Health effects of exposure to radon: BEIR VI. Vol. 6. Washington, D.C.: National Academies Press; 1999.
18. Rønning JS, Böhme M, Fredin O, Hansen L, Hermanns RL, Ofstad F, et al. Rock-avalanche deposit causes extreme high indoor radon concentrations in Kinsarvik, Ullensvang municipality, Western Norway. *Eng Geol* 2023; 321: 107136. doi: 10.1016/j.enggeo.2023.107136
19. Burghele B, Țenter A, Cucuș A, Dicu T, Moldovan M, Papp B, et al. The FIRST large-scale mapping of radon concentration in soil gas and water in Romania. *Sci Total Environ* 2019; 669: 887–92. doi: 10.1016/j.scitotenv.2019.02.342
20. Kojo K, Turtiainen T, Holmgren O, Kurttio P. Radon exposure concentrations in Finnish workplaces. *Health Phys* 2023; 125(2): 92–101. doi: 10.1097/HP.0000000000001692
21. Atyotha V, Thopan P, Fungdet S, Somtua J. Radon exhalation rates of soil samples from Khon Kaen Province, Thailand. *Mindanao J Sci Technol* 2022; 20(S1): 223–235. doi: 10.61310/mndjstmsaty.04.22
22. Wang N, Hu M, Zeng W, Yu C, Jia B, Yang Z. Indoor and outdoor Rn and Rn and their progeny levels surrounding Bayan Obo mine, China. *Nukleonika* 2020; 65(2): 145–8. doi: 10.2478/nuka-2020-0023
23. Chakraborty SR, Alam MK. Countrywide radiation dose in different locations, dwellings, and free spaces of Bangladesh. *Radiat Prot Dosimetry* 2014; 162(4): 638–48. doi: 10.1093/rpd/ncu037
24. Hasan MM, Janik M, Sakoda A, Iimoto T. Status of radon exposure in Bangladeshi locations and dwellings. *Environ Monit Assess* 2021; 193: 1–10. doi: 10.1007/s10661-021-09571-4
25. Pervin S, Yeasmin S, Khandaker MU, Begum A. Radon concentrations in indoor and outdoor environments of Atomic Energy Centre Dhaka, Bangladesh, and concomitant health hazards. *Front Nuclear Eng* 2022; 1: 901818. doi: 10.3389/fnuen.2022.901818
26. Majumder RK, Das SC, Rasul MG, Khalil MI, Dina NT, Kabir MZ, et al. Measurement of radon concentrations and their annual effective doses in soils and rocks of Jaintiapur and its adjacent areas, Sylhet, North-east Bangladesh. *J Radioanalytical Nuclear Chem* 2021; 329(1): 265–77. doi: 10.1007/s10967-021-07771-3
27. Hasan MM, Janik M, Pervin S, Iimoto T. Preliminary population exposure to indoor radon and thoron in Dhaka city, Bangladesh. *Atmosphere* 2023; 14(7): 1067. doi: 10.3390/atmos14071067
28. Roba CA, Niță D, Cosma C, Codrea V, Olah Ș. Correlations between radium and radon occurrence and hydrogeochemical features for various geothermal aquifers in Northwestern Romania. *Geothermics* 2012; 42: 32–46. doi: 10.1016/j.geothermics.2011.12.001
29. Catalano R, Mangano G, Morelli D. Radon exhalation measurements for environmental and geophysics study. *Radiat Phys Chem* 2014; 95: 349–51. doi: 10.1016/j.radphyschem.2013.02.033
30. Mohammed RS, Ahmed RS, Abdaljalil RO. Estimation of radon activity concentration in Abu Al-Khaseb and Ad Dayer soil in southern Iraq using CR-39 detector. *Environ Earth Sci* 2021; 80: 1–10. doi: 10.1007/s12665-021-09512-x
31. Soares S, Kessongo J, Bahu Y, Peralta L. Comparison of radon mass exhalation rate measurements from building materials by two different methods. *Radiat Prot Dosimetry* 2020; 191(2): 255–9. doi: 10.1093/rpd/ncaa163
32. Maeng S, Han SY, Lee SH. Analysis of radon depth profile in soil air after a rainfall by using diffusion model. *Nucl Eng Technol* 2019; 51(8): 2013–7. doi: 10.1016/j.net.2019.06.018
33. Modibo OB, Tamakuma Y, Suzuki T, Yamada R, Zhuo W, Kranrod C, et al. Long-term measurements of radon and thoron exhalation rates from the ground using the vertical distributions of their activity concentrations. *Int J Environ Res Public Health* 2021; 18(4): 1489. doi: 10.3390/ijerph18041489
34. Operation Manual RD200P2. Smart Radon Gas Monitor. Available from: https://www.radonshop.com/mediafiles/Anleitungen/Radon/FTLab_RadonEyePlus2-RD200P2/FTLab_RadonEyePlus2_ManualEN.pdf [cited 10 September 2024].
35. Dimitrova I, Georgiev S, Mitev K, Todorov V, Dutsov C, Sabot B. Study of the performance and time response of the RadonEye Plus2 continuous radon monitor. *Measurement* 2023; 207: 112409. doi: 10.1016/j.measurement.2022.112409
36. Salaheldin G, Tolba A, Kamel M, El-Taher A. Radiological hazard parameters of natural radionuclides for neoproterozoic rocks from Wadi Um Huytat in central eastern desert of Egypt. *J Radioanal Nucl Chem* 2020; 325: 397–408. doi: 10.1007/s10967-020-07262-x
37. Hanfi MY, El-Gamal H, Hussien MT, Khandaker MU, Alqahtani MS, Hasabelnaby M. Radiation doses assessment and radon exhalation rate from the soils of Albyda area, Yemen. *Nucl Eng Technol* 2025; 57(3): 103227. doi: 10.1016/j.net.2024.09.030
38. UNSCEAR. Sources, effects, & risks of ionizing radiation. Report to the General Assembly, with Scientific Annexes. New York: UN; I & II; 2000.
39. ICRP, “Summary of ICRP Recommendations on Radon,” International Commission on Radiological Protection, Jan. 26, 2018. [Online]. Available: <https://www.icrpaedia.org/images/ff/ICRPRadonSummary.pdf>

40. ICRP. International Commission on Radiological Protection for Protection against Radon at home and at work. ICRP publication 65. Oxford, UK: Pergamon Press; 1993.
41. World Health Organization. WHO handbook on indoor radon: a public health perspective. Geneva, Switzerland: World Health Organization; 2009.
42. Yang J, Busen H, Scherb H, Hürkamp K, Guo Q, Tschiersch J. Modeling of radon exhalation from soil influenced by environmental parameters. *Sci Total Environ* 2019; 656: 1304–11. doi: 10.1016/j.scitotenv.2018.11.464
43. Tchorz-Trzeciakiewicz DE, Klos M. Factors affecting atmospheric radon concentration, human health. *Sci Total Environ* 2017; 584: 911–20. doi: 10.1016/j.scitotenv.2017.01.137
44. Bossew P, Cinelli G, Ciotoli G, Crowley QG, De Cort M, Medina JE, et al. Development of a geogenic radon hazard index – concept, history, experiences. *Int J Environ Res Public Health* 2020; 17(11): 4134. doi: 10.3390/ijerph17114134
45. Singh KP, Chandra S, Panwar P, Joshi A, Prasad G, Gusain GS, et al. Measurement of radon concentration in soil gas and radon exhalation rate from soil samples along and across the Main Central Thrust of Garhwal Himalaya, India. *Environ Geochem Health* 2023; 45(11): 8771–86. doi: 10.1007/s10653-023-01758-7
46. Nuhu H, Hashim S, Aziz Saleh M, Syazwan Mohd Sanusi M, Hussein Alomari A, Jamal MH, et al. Soil gas radon and soil permeability assessment: mapping radon risk areas in Perak State, Malaysia. *PLoS One* 2021; 16(7): e0254099. doi: 10.1371/journal.pone.0254099
47. Youssef HA, Embaby AA, El-Farrash AH, Laken HA. Radon exhalation rate in surface soil of graduate's villages in West Nile delta, Egypt, using can technique. *Int J Recent Sci Res* 2015; 6(4): 3440–6.
48. Alharbi WR, Abbadly AG. Measurement of radon concentration in soil and the extent of their impact on the environment from Al-Qassim, Saudi Arabia. *Natural Science* 2013; 5(1): 93–98. doi: 10.4236/ns.2013.51015
49. Al-Gharabi M, Al-Hamzawi A. Measurement of radon concentrations and surface exhalation rates using CR-39 detector in soil samples of Al-Diwaniyah Governorate, Iraq. *Iran J Med Phys* 2020; 17(4): 220–4. doi: 10.22038/IJMP.2019.40303.1552
50. Duggal V, Rani A, Mehra R. Measurement of soil-gas radon in some areas of northern Rajasthan, India. *J Earth System Sci* 2014; 123: 1241–7. doi: 10.1007/s12040-014-0473-5
51. Tawfiq NF, Mansour HL, Karim MS. Radon gas concentrations in soil and radon exhalation rates in Thiqr City. In 2nd Conference on Environment and Sustainable Development 28-29-Oct-2015. *Eng. & Tech. Journal*, 2016; Vol. 34, Part (B), No. 3: 434–443. doi: 10.30684/etj.34.3b.11
52. Zebalah KJ, Sh Aswood M, Showard AF. Distribution of radon concentration in agricultural soil samples in AL-Qadisiyah, Iraq. *J Pharm Negat Results* 2022; 13(4): 1251–8.
53. Deeba F, Rahman SH, Kabir MZ. Radon concentration in soil and groundwater of west coastal area, Bangladesh. *Radiat Prot Dosim* 2020; 191(3): 341–8. doi: 10.1093/rpd/ncaa134
54. Deeba F, Rahman SH, Kabir MZ, Dina NT. Annual effective dose due to ²²²Rn and evaluation of ²³⁸U, ²³²Th, and ⁴⁰K contents in soil at the south-eastern coastal area of Bangladesh. *J Radioanal Nucl Chem* 2022; 331(2): 817–26. doi: 10.1007/s10967-021-08169-x

***Sopan Das**

Atomic Energy Centre, Chattogram
 Bangladesh Atomic Energy Commission
 1018/A Bayezid Bostami Road, East Nasirabad,
 Chattogram - 4209
 Email: sopandas@yahoo.com